CONFERENCE PRE-PRINT

FIRST EXPERIMENTAL OBSERVATION OF "STAIRCASE" HIGH CONFINEMENT MODE IN TOKAMAK PLASMA

Y. ZHANG, Y. R. ZHU, G. Q. DONG, Z. J. LI, Z. WANG, Y. F. LIU, Y. J. ZHOU, X. X. HE, S. S. YANG, Y. Q. SHEN, S. B. GONG, X. YU, R. KE, M. JIANG, Z. Wang, T. F. SUN, Y. H. CHEN, J. B. YUAN, A. S. LIANG, Z. Y. YIN, G. Z. HAO, L. XUE, J. Q. LI, G. L. XIAO, Z. B. SHI, B. LI, W. CHEN, W. L. ZHONG and HL-3 TEAM

Southwestern Institute of Physics, Chengdu 610041, China

Email: zhangyi@swip.ac.cn

Z. B. GUO and M. XU Fudan University, Beijing 100871, China

C. LI and Y. H. WANG Peking University, Beijing 100871, China

X. G. Wang Harbin Institute of Technology, Harbin 150006, China

Y. F. WANG Institute of Plasma Physics, Chinese Academy of Sciences, Hefei 230031, China

Z. Y. LI General Atomics, San Diego 85608, CA, USA

Abstract

We report the first unambiguous experimental realisation of a stable, edge-localised-mode (ELM)-free "staircase H-mode" (SCH-mode) on the HL-3 tokamak. Instead of relying on a single, steep pedestal, the discharge evolves a spatially periodic, mesoscale ion temperature corrugation that spans the entire minor radius. Each staircase step comprises a weak-gradient platform and a narrow jump layer; the combined structure distributes the free energy that ordinarily drives giant ELMs into multiple, individually stable layers. Linear stability analyses confirm that the edge pressure and current gradient in the jump layer is kept below the peeling-ballooning boundary for the SCH-mode. The SCH-mode is distinguished from other ELM-free regimes by the absence of quasi-coherent modes (QCM), weakly coherent modes (WCM), edge harmonic oscillations (EHO) or broadband edge fluctuations. The resulting avalanche-like transport in the flat region exhausts edge power continuously, eliminating large, transient heat loads. The mode is sustained for 0.4s without external magnetic perturbations, pellet pacing or dedicated impurity seeding, and achieves $\beta_N \approx 1.8$ and $H_{98,y2} \approx 1.1$. The SCH-mode favors low collisionality and therefore offers an intrinsically robust, hardware-simple route to ELM-free, reactor-relevant high confinement.

1. INTRODUCTION

The ultimate goal of magnetic-confinement fusion is to ignite a deuterium—tritium plasma that produces more energy than it consumes. In a tokamak this requires simultaneously achieving high temperature, sufficient density and long energy-confinement time. Over four decades of experimental progress, the high-confinement mode (H-mode) has emerged as the default scenario for the next-step device ITER [1] and for the demonstration power plant DEMO [2]. First observed on ASDEX in 1982 [3], H-mode is characterised by an edge transport barrier—a narrow pedestal of steep pressure gradient—that suppresses micro-turbulence [4] and boosts global confinement by roughly a factor of two compared with the low-confinement (L-mode) state [5]. The pedestal, however, is intrinsically fragile. As the pressure gradient increases to meet fusion performance requirements, ideal magnetohydrodynamic (MHD) instabilities are driven, most notably the peeling—ballooning (P-B) mode [6], which erupts explosively as an edge-localised mode (ELM) [7]. Type-I ELMs expel up to 20 % of the plasma stored energy in a millisecond [8], imposing instantaneous heat loads on plasma-facing components that exceed 10 MW m⁻² in ITER-scale devices [9]. Such transients threaten the lifetime of divertor targets and first-wall materials, and may ultimately determine the duty cycle and availability of a fusion power plant [10].

The fusion community has therefore pursued two complementary strategies to mitigate or eliminate ELMs. The first is active control: external coils apply resonant magnetic perturbations (RMP) to tear open magnetic islands

at the pedestal foot, thereby flattening the pressure gradient and releasing energy in a controlled fashion [11]. While RMP has demonstrated partial success on DIII-D [12], JET [13] and EAST [14], it demands sophisticated 3-D coil sets and real-time feedback, and may degrade core confinement or trigger secondary locked modes [15]. Pellet pacing [16], vertical kicks [17] and impurity seeding [18] have also been explored, but each adds hardware complexity and introduces new failure modes.

The second strategy is passive control: identify new regions of operational space where the pedestal is intrinsically stable, yet high confinement is preserved. This led to the discovery of several "soft" H-mode variants—EDA [19], I-mode [20], QH-mode [21] and QCE [22]—each characterised by benign edge relaxation dynamics. EDA H-mode, first observed on Alcator C-Mod [19], exhibits a quasi-coherent mode (QCM) in the 50–150 kHz range that continuously expels particles and heat, preventing the pressure gradient from reaching the P-B limit. I-mode replaces the sharp pedestal with a weak density barrier and a weakly coherent mode (WCM) that flushes impurities while maintaining good energy confinement [20]. QH-mode relies on an edge harmonic oscillation (EHO) driven by high β and strong rotation to broaden the pedestal and release energy in small, regular bursts [21]. Quasi-continuous exhaust (QCE) further reduces ELM size by operating at high separatrix density, $n_{e,sep} \gg 0.3 n_{GW}$ (here n_{GW} is the Greenwald density limit), where small, high-frequency ELMs dominate [22]. Despite their success, these regimes are not universally accessible: EDA demands high collisionality [19], QH requires elevated toroidal rotation [21], and QCE needs dense edge plasmas that may complicate fuel purity and divertor detachment [22].

Against this backdrop, theoretical and computational studies have long predicted an alternative route to ELM-free confinement: the "staircase" profile [23–27]. In a staircase, the steep pedestal is replaced by a periodic, mesoscale corrugation of the pressure profile consisting of alternating weak-gradient platforms and strong-gradient jumps [28]. The free energy that would otherwise accumulate in a single edge layer is distributed over several jumps, each individually below the P-B threshold [29]. Micro-turbulence within each platform is regulated by zonal-flow shear [30], leading to avalanche-like transport that continuously exhausts power without large collapses [31]. Early gyrokinetic simulations revealed staircase formation under low-collisionality conditions and sufficient magnetic shear [32], but experimental evidence remained elusive. Transient staircases were reported in L-mode plasmas on HL-2A [33] and KSTAR [34], and RMP-driven staircase pedestals were observed on DIII-D [35], yet none sustained a stable H-mode for longer than a few milliseconds.

The present work reports the first unambiguous experimental realisation of a stationary, ELM-free "staircase H-mode" (SCH-mode) on the HL-3 tokamak. HL-3 (formerly known as HL-2M) is currently the largest tokamak device in China, with major radius R=1.78 m, minor radius a=0.65 m and maximum plasma current $I_p=3MA$. [36]. The device allows flexible shaping up to $\kappa\approx 1.9$ and $\delta\approx 0.8$ [36]. In 2023, HL-3 successfully operated in H-mode with a plasma current of one million amperes for the first time in China [37]. The HL-3 serves critical roles in supporting the operation of ITER and aiding the design of future fusion devices by integrating both technological and physics advancements. The primary missions of the HL-3 include, but are not limited to: (1) Testing and qualifying various advanced divertor concepts, addressing both physics and technological aspects. (2) Testing and validating high heat flux plasma-facing components. (3) Investigating burning plasma physics and designing scenarios compatible with advanced divertor configurations.

2. EXPERIMENTAL SET-UP

All results reported here were obtained on the HL-3 tokamak. The discharges described in this paper used a lower single-null divertor geometry with the basic plasma parameters: plasma current $I_p = 0.5MA$, toroidal magnetic field $B_T = 1.54T$, upper triangularity $\delta_u = 0.35 - 0.55$, lower triangularity $\delta_l = 0.7$, and $q_{95} = 5.26$.

Plasmas were heated by a combination of neutral-beam injection (NBI) and electron-cyclotron resonance heating (ECRH). Four positive-ion NBI sources injected up to 1.2 MW of 45 keV deuterium tangentially in the co-current direction, while 105 GHz gyrotrons supplied 1.4 MW of ECRH. The total injected power (≈ 2.6 MW) was chosen to remain close to the empirical L $^-$ H power threshold so that the formation of the staircase H-mode (SCH-mode) could be attributed to profile optimisation rather than to a large power overshoot.

Line-averaged electron density was measured with FIR diagnostics. Electron temperature and density profiles were obtained from core and edge Thomson scattering system, with a time resolution of (20–30) ms and spatial resolution of (1.2–1.5) cm. Ion temperature and toroidal rotation profiles were derived from C⁶⁺ charge-exchange recombination spectroscopy (CXRS). The CXRS system provides 32 radial channels with a time resolution of 50 ms and spatial resolution of (1.0–2.5) cm. Beam-emission spectroscopy (BES) with 32 radial channels was

employed to measure density fluctuations at 2 MHz sampling; the radial resolution is ≈ 1.8 cm and the poloidal resolution ≈ 1.5 cm. Frequency-modulated continuous-wave (FMCW) reflectometry was used to reconstruct the edge electron density profile.

Magnetic equilibrium was reconstructed using kinetic-EFIT constrained by 40 poloidal flux loops. Mirnov coils were used to monitor MHD activity. Experimental data were analysed off-line using the OMFIT integrated modelling framework.

3. OBSERVATION OF THE SCH-MODE

The first experimental confirmation of a stable, ELM-free "staircase H-mode" (SCH-mode) on HL-3 is documented in this section. The discharge #6580 forms the core data set. Below, we present the global evolution, pedestal and staircase formation, stability analysis and distinction from established ELM-free regimes, respectively.

3.1. Global temporal evolution

Figure 1 (a–g) summarises the typical shot #6580 of the SCH-mode on HL-3. The plasma current was ramped to $I_p=0.5$ with the upper triangularity $\delta_U=0.55$. ECRH (1.4 MW, 105 GHz) was applied at t = 1150ms while NBI (1.2 MW, 45 keV) remained constant during t=1000-2000ms. The line-averaged density \bar{n}_e rose from $1.0\times10^{19}\,\mathrm{m}^{-3}$ to $2.0\times10^{19}\,\mathrm{m}^{-3}$ within 200 ms and stayed constant thereafter. The stored energy W_E , climbed from 0.12 MJ (L-mode) to 0.18 MJ within 150 ms and saturated at 0.18 MJ, giving a normalised $\beta_N\approx1.3$. Concurrently, the H-factor $H_{98,y2}$ increased from 0.9 to 1.1. The absence of ELMs persisted for 400ms (1320ms–1720ms), after which ECRH was ramped down in 100 ms. The discharge reverted to L-mode accompanied by only two minor D_α bursts compared to the large ELM amplitude observed in an ELMy H-mode (#6579), indicating a benign energy release.

For comparison, Fig. 1 also overlays a standard type-I ELMy H-mode (#6579) with the same lower triangularity ($\delta_L = 0.7$), smaller upper triangularity ($\delta_U = 0.35$) and slightly larger NBI heating power (1.5MW). In #6579, periodic ELMs are represented by large D_{α} spikes. The dramatic reduction of transient heat loads in #6580 is the first qualitative signature of the SCH regime.

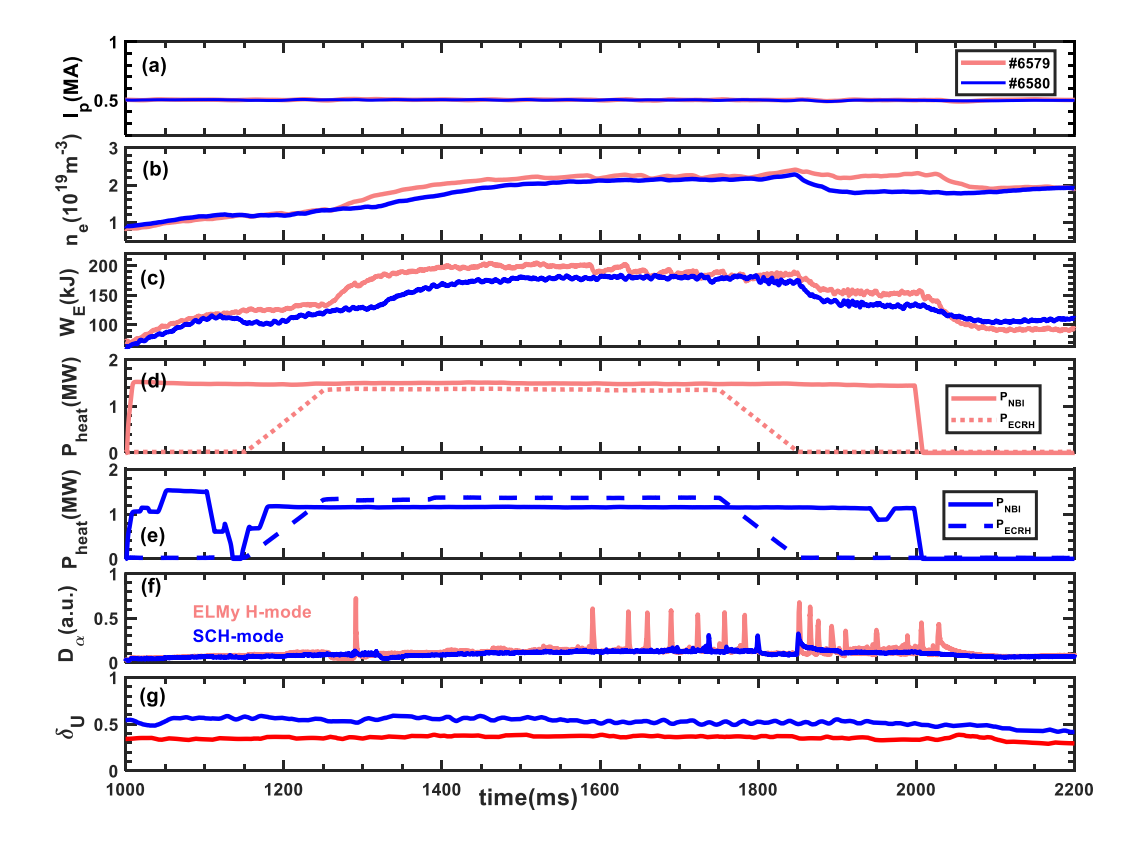


FIG. 1. Comparison of time history of plasma parameters in two shots, one is ELMy H-mode (#6579) and another is SCH-mode (#6580): (a) the plasma current I_p ; (b) the line-averaged plasma density; (c) the plasma stored energy; (d) and (e) are the injected heating power by NBI and ECRH for #6579 and #6580, respectively; (f) and (g) are the the D_{α} radiation signals for #6579 and #6580, respectively; the upper triangularity is $\delta_u = 0.35$ for #6579 and $\delta_u = 0.55$, respectively. the lower triangularity is $\delta_i = 0.70$ for both #6579 and #6580.

3.2. Pedestal and staircase formation

Figure 2 displays the ion temperature (T_i) profiles measured by CXRS at two characteristic times. The red data points and curve represent the ELMy H-mode profile, characterized by a steep temperature gradient near the Last Closed Flux Surface (LCFS) and a relatively smaller gradient within the core plasma. In contrast, the blue data points and curve depict the SCH-mode profile, distinguished by pronounced "steps" along the radial direction, indicative of discrete steep gradient regions. It can be clearly observed that the T_i profile exhibits a staircase structure, spanning the whole radial range of $0 < \rho < 1$. Each step comprises a weak-gradient platform separated by a strong-gradient jump. The maximum gradient in the edge region is smaller than that of the ELMy H-mode. It should be mentioned that the upper triangularity of the SCH-mode is larger than that of the ELMy H-mode, as illustrated by the dashed curves in figure 2.

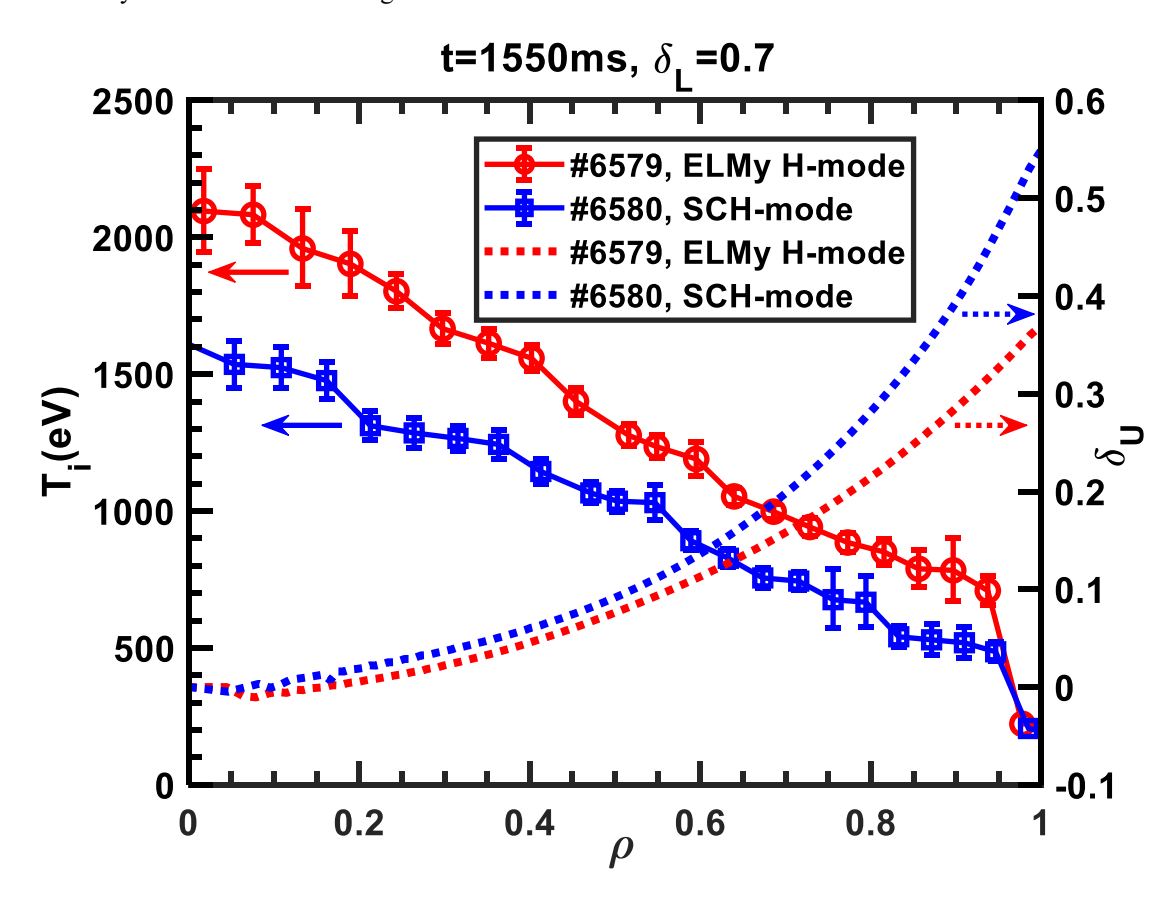


FIG. 2. The typical ion temperature profiles with respected to ELMy H-mode and SCH-mode. Here the markers with error bars denote the measured data, the solid lines denote fitted profiles and the dashed lines denote upper triangularity. The lower triangularity is fixed as $\delta_{L,LCFS} = 0.7$.

3.3. Stability analysis

To understand why the SCH-mode remains free of type-I ELMs for hundreds of millisecond, we performed a comprehensive stability assessment covering peeling-ballooning (P-B) modes by means of the ELITE code. The analysis use profiles reconstructed by kinetic-EFIT. The P-B mode is the canonical driver of type-I ELMs. Its growth rate γ scales with the normalized edge pressure gradient α and the edge current density $(j_{max} + j_{sep})/(2\langle j \rangle)$, where $\alpha = -(2\mu_0 Rq^2/B^2) \nabla p$ and j is the current density. We employed the ELITE code coupled to

kinetic-EFIT within the OMFIT framework to compute γ based on the equilibrium of shots #6580 at t = 1550ms. Figure 3 displays the stability map in the α -j plane, and the contour $\gamma/(\omega_i^*/2) = 1$ defines the marginal stability boundary, with ω_i^* the ion diamagnetic frequency.

For the SCH-mode (#6580), the operating point lies deep inside the stable region. The staircase structures distributes the equilibrium pressure into several mesoscale jumps, reducing the maximum local α . Consequently, the edge bootstrap current density drops, placing the discharge well below the peeling boundary. The absence of any excursion into the unstable region in #6580 explains the observed ELM quiescence.

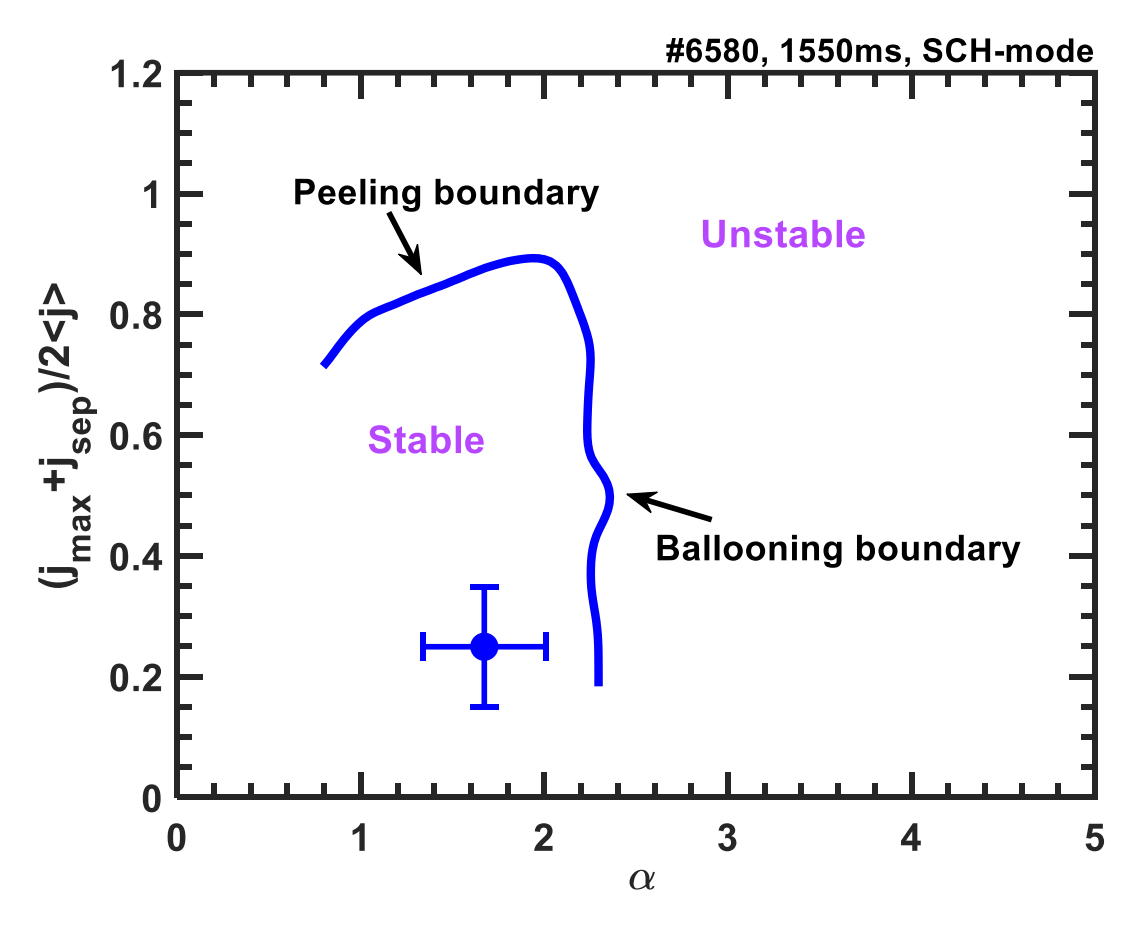


FIG. 3. Edge peeling-ballooning instability analysis in the normalized pressure gradient (α) and current density ($(j_{max} + j_{sep})/(2\langle j \rangle)$) plane. The stability boundaries are defined as $\gamma/(\omega_i^*/2) = 1$, where γ is the growth rate of the most unstable mode and ω_i^* is the ion diamagnetic frequency.

3.4. Distinction from established ELM-free regimes

The SCH-mode occupies a distinct niche in the landscape of ELM-free high-confinement scenarios. Unlike the EDA H-mode, which thrives under high collisionality ($\nu_e^* > 1.5$, where $\nu_e^* = 6.921 \times 10^{-18} (qRn_eZ\ln\Lambda_e)/(T_e^2\epsilon^{3/2})$, with $\ln\Lambda_e = 31.3 - \ln(\sqrt{n_e}/T_e)$ and $q, R, n_e, T_e, Z, \epsilon$ being the safety factor at 95% of flux surface, major radius in m, electron density at the pedestal top in m^{-3} , electron temperature at the pedestal top in eV, effective ion charge, inverse aspect ratio, respectively.) and is always linked to an edge quasi-coherent mode (QCM) detected by BES and reflectometry. The SCH-mode is accessed at low collisionality ($\nu_e^* < 1.0$) and shows no trace of QCM in the BES spectra, as shown in figure 4.

Additionally, the absence of a weakly coherent mode (WCM) further distinguishes it from I-mode, where WCM is a defining feature. QH-mode, on the other hand, relies on edge harmonic oscillations (EHO) or broadband turbulence to flush power continuously. In SCH discharges the operational point lies deep inside the stable region of peeling–ballooning stability diagrams, no EHO or broadband edge turbulence is observed, and the edge remains quiescent for hundreds of millseconds. Apart from that, Quasi-continuous exhaust (QCE) requires a high

separatrix density $n_{e,sep} \ge 0.3 \times n_{GW}$ (where n_{GW} is the Greenwald density limit) to maintain small-ELM dynamics. Our measurements give $n_{e,sep} = 0.09 n_{GW} \ll 0.3 n_{GW}$, well below the QCE threshold.

These combined diagnostics—collisionality, spectral content, stability location and separatrix density—establish the SCH-mode as a new, intrinsically stable, coherent-mode-free branch of ELM-free H-mode, characterised by a mesoscale staircase pressure profile and benign, avalanche-like edge power exhaust.

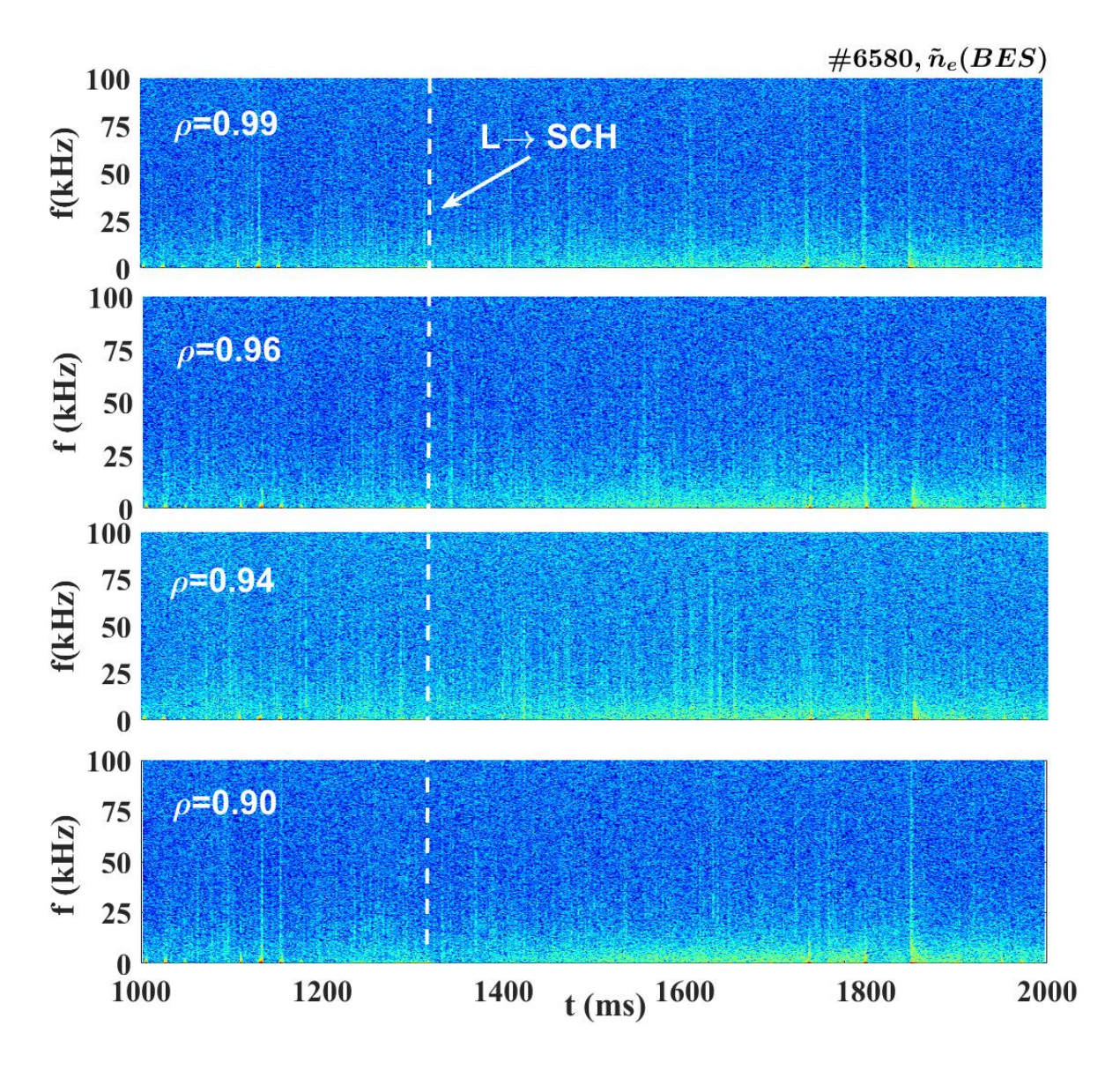


FIG. 4. The spectrogram of the density perturbations measured by BES at different radial locations.

4. DISCUSSION AND CONCLUSIONS

Our experiments provide the first unambiguous demonstration that a mesoscale staircase profile can sustain a high-confinement, ELM-free regime in a tokamak. The SCH-mode is achieved without external coils, resonant perturbations or dedicated particle pacing, indicating that the stabilisation mechanism is intrinsic to the self-organised pressure corrugation. Stability analyses show that distributing the free energy over several mesoscale layers lowers the local pressure gradient below the peeling–ballooning threshold, while residual micro-turbulence is regulated by zonal-flow shear inside each jump layer. The result is a continuous, avalanche-like heat exhaust that removes edge power without large collapses. Scaling considerations suggest that the regime remains accessible at reactor-relevant parameters. The empirical window $v_e^* < 1.0$ comfortably overlaps the ITER baseline collisionality.

Future work will extend the database to higher β_N and longer pulses, quantify isotope and rotation dependencies, and develop real-time profile-control algorithms to lock the staircase structure actively. If confirmed on larger devices, the SCH-mode could provide a simple, robust path to ELM-free operation for DEMO and commercial fusion reactors.

ACKNOWLEDGEMENTS

The authors thank the HL-3 operation and engineering teams. This work was supported by the National MCF Energy R&D Programme (2024YFE03270400, 2022YFE03010004, 2022YFE03060003), NSFC (1205013, 12405256, 12075079, 12375210), Sichuan NSF (2023NSFSC1290, 2022JDRC0014) and SWIP Innovation Programme (202301XWCX001-02).

REFERENCES

- [1] ITER PHYSICS EXPERT GROUPS, ITER Physics Basis, Nucl. Fusion 39 (1999) 2137–2664.
- [2] ROMANELLI, F., et al., DEMO Design Basis 2015, Nucl. Fusion 55 (2015) 043003.
- [3] WAGNER, F., et al., Regime of improved confinement and high beta in neutral-beam-heated divertor discharges of the ASDEX tokamak, Phys. Rev. Lett. 49 (1982) 1408–1412.
- [4] DIAMOND, P.H., et al., Zonal flows in plasma—a review, Plasma Phys. Control. Fusion 47 (2005) R35-R161.
- [5] MARTIN, Y., et al., Energy confinement and MHD activity in JET ELMy H-modes, Nucl. Fusion 48 (2008) 065004.
- [6] CONNOR, J.W., Edge-localized modes—physics and theory, Plasma Phys. Control. Fusion 40 (1998) 531-542.
- [7] LEONARD, A.W., Edge-localized modes in tokamaks, Phys. Plasmas 21 (2014) 090501.
- [8] LOARTE, A., et al., Characteristics of type-I ELM energy and particle losses in JET and their extrapolation to ITER, Plasma Phys. Control. Fusion 47 (2005) S203–S229.
- [9] PITTS, R.A., et al., Material migration and erosion in ITER, J. Nucl. Mater. 438 (2013) S48-S56.
- [10] FEDERICI, G., et al., Key ITER plasma edge and divertor issues, Nucl. Fusion 41 (2001) 1967-1977.
- [11] EVANS, T.E., et al., Suppression of large edge localized modes with edge resonant magnetic fields in high confinement DIII-D plasmas, Nat. Phys. 2 (2006) 419–423.
- [12] FENSTERMACHER, M.E., et al., ELM suppression using magnetic perturbation coils on DIII-D, Phys. Plasmas 15 (2008) 056122.
- [13] SUTTROP, W., et al., Experimental studies of edge localized mode mitigation by resonant magnetic perturbations in ASDEX Upgrade, Phys. Rev. Lett. 106 (2011) 225004.
- [14] LIANG, Y., et al., Active control of type-I edge localized modes with n = 1 and n = 2 magnetic perturbations on EAST, Phys. Rev. Lett. 110 (2013) 235002.
- [15] PAZ-SOLDAN, C., et al., Locked mode threshold scaling in DIII-D with applied 3D fields, Phys. Rev. Lett. 114 (2015) 255001.
- [16] BAYLOR, L.R., et al., Pellet pacing of edge localized modes in DIII-D, Phys. Plasmas 18 (2011) 056112.
- [17] DE LA LUNA, E., et al., Vertical kicks for ELM mitigation in JET ILW, Nucl. Fusion 57 (2017) 126038.
- [18] FRERICHS, H., et al., Impurity seeding for ELM mitigation in ASDEX Upgrade, Nucl. Fusion 60 (2020) 046013.
- [19] HUBBARD, A.E., et al., EDA H-mode studies on Alcator C-Mod, Phys. Plasmas 14 (2007) 056115.
- [20] WHYTE, D.G., et al., I-mode: an H-mode energy confinement regime with L-mode particle transport, Nucl. Fusion 50 (2010) 105005.
- [21] BURRELL, K.H., et al., Quiescent H-mode plasmas in DIII-D, Plasma Phys. Control. Fusion 44 (2002) A253-A261.
- [22] HARRER, G.F., et al., Quasicontinuous exhaust scenario for a fusion reactor, Phys. Rev. Lett. 129 (2022) 165001.
- [23] DIF-PRADALIER, G., et al., On the validity of the local diffusive paradigm in turbulent plasma transport, Phys. Rev. E 82 (2010) 025401(R).
- [24] WANG, W., et al., A mechanism for the formation and sustainment of the self-organized global profile and E×B staircase in tokamak plasmas, Nucl. Fusion 58 (2018) 056005.
- [25] YAN, Q.H., DIAMOND, P.H., Staircase formation by resonant and non-resonant transport of potential vorticity, Nucl. Fusion 62 (2022) 126032.
- [26] RAMIREZ, F.R., DIAMOND, P.H., Staircase resiliency in a fluctuating cellular array, Phys. Rev. E 109 (2024) 025209.
- [27] KOSUGA, Y., et al., How the propagation of heat-flux modulations triggers E×B flow pattern formation, Phys. Rev. Lett. 110 (2013) 105002.

- [28] DIF-PRADALIER, G., et al., Finding the elusive E×B staircase in magnetized plasmas, Phys. Rev. Lett. 114 (2015) 085004.
- [29] HAHM, T.S., DIAMOND, P.H., Mesoscopic transport events and the breakdown of Fick's law for turbulent fluxes, J. Korean Phys. Soc. 73 (2018) 747–792.
- [30] ASHOURVAN, A., DIAMOND, P.H., How mesoscopic staircases condense to macroscopic barriers in confined plasma turbulence, Phys. Rev. E 94 (2016) 051202.
- [31] POLITZER, P.A., Observation of avalanche-like phenomena in a magnetically confined plasma, Phys. Rev. Lett. 84 (2000) 1192–1195.
- [32] WANG, W., et al., Statistical study for ITG turbulent transport in flux-driven tokamak plasmas, Nucl. Fusion 60 (2020) 066010.
- [33] LIU, W., et al., Evidence of E×B staircase in HL-2A L-mode tokamak discharges, Phys. Plasmas 28 (2021) 012512.
- [34] CHOI, M.J., et al., Mesoscopic transport in KSTAR plasmas: avalanches and the E×B staircase, Plasma Phys. Control. Fusion 66 (2024) 065013.
- [35] ASHOURVAN, A., et al., Formation of a high-pressure staircase pedestal with suppressed edge localized modes in DIII-D, Phys. Rev. Lett. 123 (2019) 115001.
- [36] DUAN, X.R., et al., Progress of HL-2A experiments and HL-2M program, Nucl. Fusion 62 (2022) 042020.
- [37] ZHONG, W.L., et al., China's HL-3 tokamak achieves H-mode operation with 1 MA plasma current, The Innovation 5 (2024) 100555.